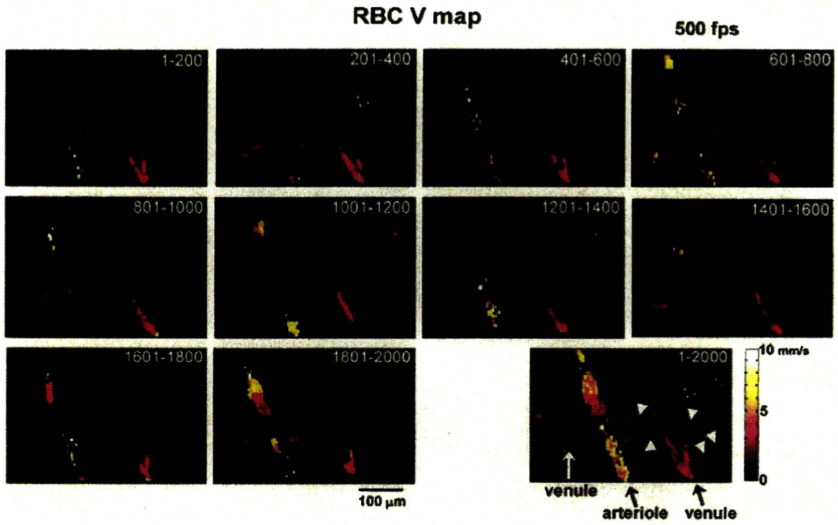

Fig. 5. Sequential RBC velocity (V) maps in a capillary network, 0.4 s apart. These maps were obtained from the identical ROI of the same rat as Fig. 4. Capillaries are shown by white arrowheads. Note the color heterogeneity, which represents different speeds of the same RBC in a single capillary (ranging from 0.33 to 2.60 mm/s), in an arteriole (ranging from 3.44 to 8.22 mm/s) and in venules (ranging from 1.27 to 4.52 mm/s).

attachments of astroglial elements to the vein are seen. RBCs in the vein are clearly visible in yellow color; some have a round shape and others are rather elongated. Panel B shows a longitudinal section of an arteriole of approximately 50 μm in diameter. There is a thick layer of astroglial endfeet colored brown and incompletely stained endothelial layers in green constituting the glio-vascular interface, where the Virchow–Robin space must exist. Because of the poor spatial resolution, we carefully illustrated the images and surmised a broad structural interrelationship between astroglial elements and the arteriole in which astroglia form a complete, thinly spread, continuous covering on the arteriolar surface, with a holding-type or synaptic-type *en face* contact with the vessel wall, as roughly illustrated in the right panel of the upper row. The lower row of Fig. 3 shows the interrelationship between a single capillary, glial endfeet and RBC movements at intervals of 10 s. There seem to be scanty synaptic-type or holding-type attachments of astroglial endfeet on the capillary surface. However, it should be noted that the absence of a brown-colored sheath around capillaries does not necessarily imply the absence of "membrane limitans gliae superficialis," as observed by electron-microscopy (Wolf, 1970). It seems likely that the astroglial endfeet layer covering capillaries would be too thin to hold the staining material.

Control RBC movements as viewed with high-speed video

As mentioned before, when FITC-labeled RBCs were injected into the circulating blood, they appeared in the cerebral microvasculature as bright circles against a dark background with the high-speed camera laser-scanning confocal fluorescence microscope. The program identified the vast number of RBCs as above-threshold light intensity features (Fig. 1), recognized their positions (centroids) in *x*–*y* coordinates frame by frame for the selected number of frames, and stored the data in the PC (Supplemental movie 1). Fig. 4 shows all RBCs that were detected in the visual field for 2000 frames (4 s). This map represents the fundamental data for this study. The numbers on the map define the order of appearance of RBCs, shown in different colors. From the data, the velocities of all RBCs were calculated based

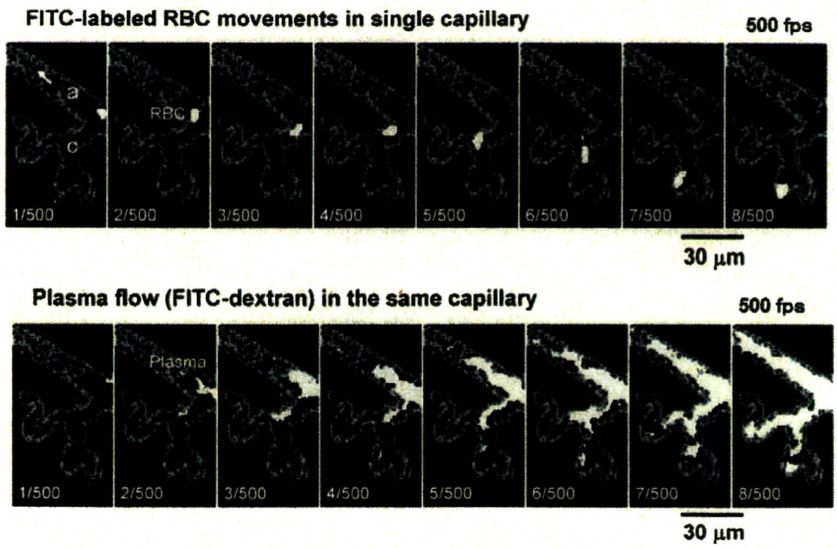

Fig. 6. To show RBC flow at 500 fps (top) in an arteriole (a) and a single capillary (c) and plasma flow (bottom) after intra-carotid injection of FITC-dextran. The frame intervals are 1/500 s (see text for further explanation).

Please cite this article as: Tomita, M., et al., Oscillating neuro-capillary coupling during cortical spreading depression as observed by tracking of FITC-labeled RBCs in single capillaries, NeuroImage (2011), doi:10.1016/j.neuroimage.2011.02.078

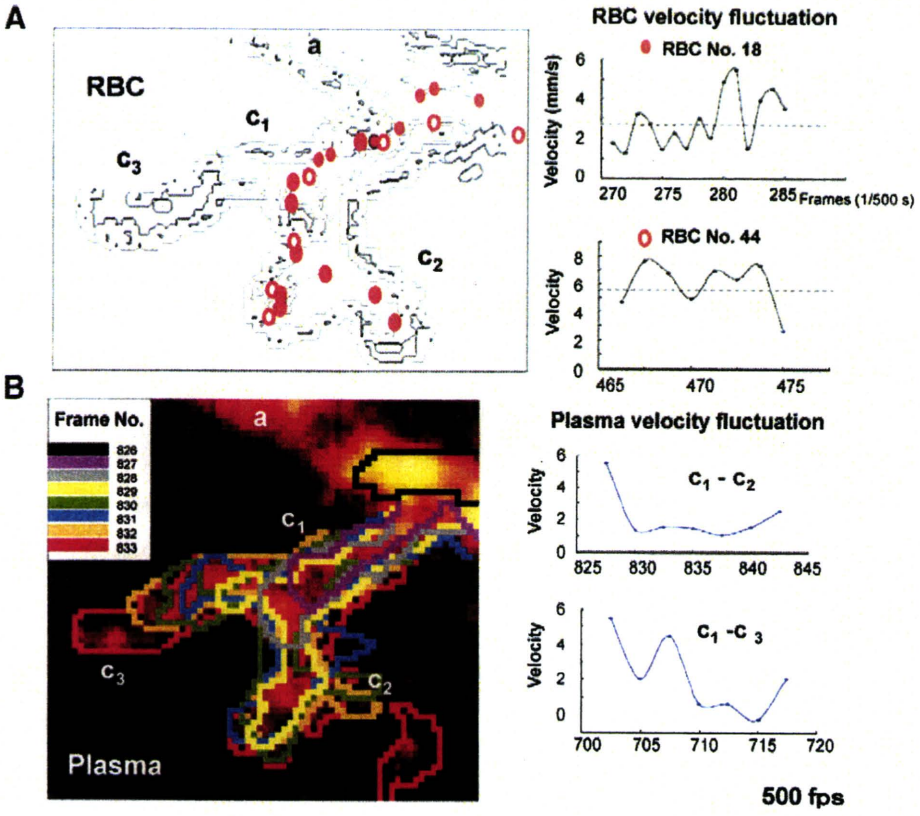

Fig. 7. More comprehensive analysis of the data shown in Fig. 6. Movements of two RBCs (A) in a specified period occurred in the capillary c2. In (B), contour changes of FITC-dextran were traced every 1/500 s in different colors, showing that a very variable diffusion process occurs at the boundary. The right panels of the two columns show the velocities of RBCs and plasma plotted against time in seconds. The synchronous fluctuations suggest that very complex vasomotion was occurring in the capillaries, which lack muscle cells.

on the displacement distance (μm) per frame multiplied by the frame rate (500 per second in this case), affording a velocity map (V map), and a topographical RBC number map for a specified period (RBC N map). Off-line analysis was required to separate RBCs in capillaries, since the figure contained all RBCs appearing even in arterioles and veins, and the computer cannot discriminate the vessels. Capillaries were identified by comparing the obtained maps and a movie recorded with a conventional video system. Fig. 5 is the V map of

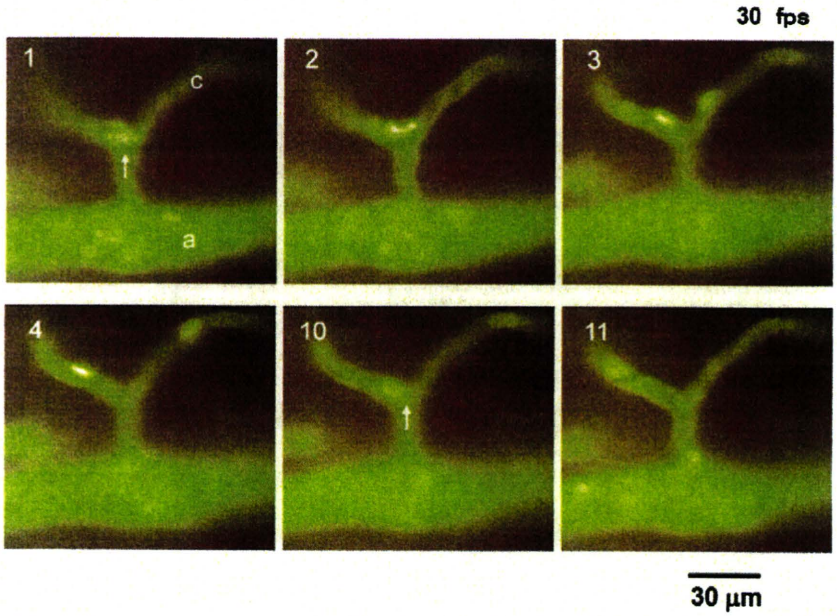

Fig. 8. Unpredictable left–right distribution of RBCs at a capillary branch. Two RBCs at the point of bifurcation separated and moved in opposite directions at frames 1, 2, 3 and 4 (30 fps) in the absence of any detectable change in diameter of capillary. Another RBC came at frame 10 and proceeded to the left capillary, again without any apparent change in diameter. These results seem inconsistent with the involvement of a putative capillary sphincter.

Please cite this article as: Tomita, M., et al., Oscillating neuro-capillary coupling during cortical spreading depression as observed by tracking of FITC-labeled RBCs in single capillaries, NeuroImage (2011), doi:10.1016/j.neuroimage.2011.02.078

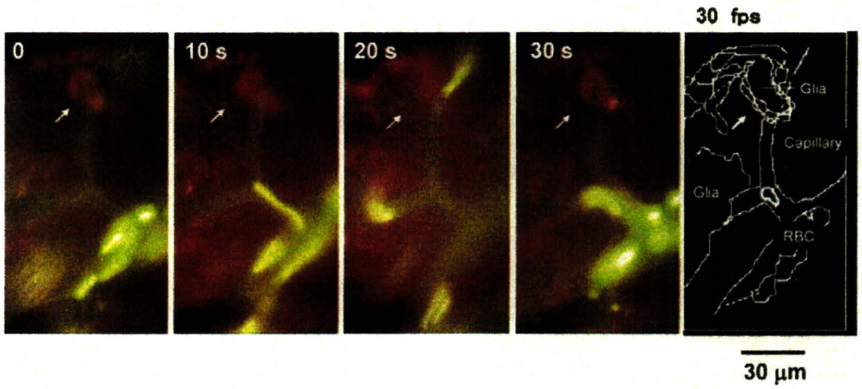

Fig. 9. Morphological changes of astroglial soma and endfeet over 30 s. An illustration of the cumulative morphological changes of the astroglial elements is shown in the right panel (arrow).

RBCs in microvessels obtained from the same motion picture as used for Fig. 4, showing the time-to-time changes in velocity of RBCs in a limited region, in sequences of 200 frames each, i.e., 1–200 (0.4 s), 201–400 (0.4 s), 401–600 (0.4 s).....1801–2000 (0.4 s). It should be noted that movements of RBCs are heterogeneous, not stationary, presumably reflecting local neuronal requirements, in line with previous reports that RBC flow in single capillaries continuously fluctuated within a limited range in rats and mice (Unekawa et al., 2008; Unekawa et al., 2010).

Fig. 6 shows a capillary in which an RBC is moving at intervals of 1/500 s in the upper row, together with plasma flow traced with FITC-dextran in the same capillary, on the same time scale. Note that plasma flow was also heterogeneous; indeed, the calculation of average plasma velocity was difficult because parts of the diffusion front moved faster while others moved slower, as analyzed in Fig. 7. In the lower panel, contours of plasma dispersion are traced at every 1/500 s. Both RBC flow and plasma flow showed rather high-frequency fluctuations (see the right panels). Evaluation with KEIO-IS2 yielded a value of RBC velocity in single capillaries of 2.00 ± 1.56 mm/s (mean $\pm$ SD, $n = 5$, at 500 fps) whereas a somewhat lower velocity of 1.80 ± 2.01 mm/s (mean $\pm$ SD, $n = 5$) was obtained for plasma propagation in the identical capillaries. Chronological plots of sequential RBC and plasma velocities revealed high-frequency fluctuation in 2 capillaries. These observations may contribute to efforts to understand the hemodynamic mechanisms of RBC flow in capillaries.

RBC distribution at capillary branching sites was simply unpredictable. Fig. 8 shows the left–right distribution of RBCs at a capillary branch. Two RBCs reached the branch at the first frame, separated, and moved off in opposite directions at the 2nd, 3rd and 4th frames (30 fps). There was no detectable change in the diameter of the capillary. At the 10th frame, another RBC arrived at the branch and proceeded into the left capillary, again without any apparent change in the diameter of the capillary. There was no indication of any role of a capillary sphincter, if such a structure exists (Nakai et al., 1981), leaving open the possibility that a transient plasma viscosity change directs RBCs to the pertinent capillary. Fig. 9 illustrates the slow morphological changes of astroglial endfeet, which covered a branch of the capillary at the periphery, every 10 s. RBCs, stained yellow, appeared elongated in the 30 fps video images. However, no direct correlation between the morphological changes and RBC velocity was apparent, although this phenomenon might reasonably have been expected.

RBC movements during CSD

RBC movements in single capillaries during CSD elicited by K^+ microinjection were observed to decrease gradually, with or without an initial transient increase, employing the same apparatus as used for the control study, except for the use of slow-speed video for the estimation of background darkness and the detection of slowing RBCs. The RBC velocity decreased in a fluctuating fashion and finally stopped at 6 min after the onset of CSD in this case while in other cases, RBCs disappeared from the local capillary network (Fig. 10 upper images and Supplemental movie 2). We found that RBC velocity decreased to nearly 0 in 5 out of 10 rats, and reversed RBC flow was seen in 3 out of 10 rats. Increasing neuronal depolarization during CSD was estimated from the darkness of the tissue background. However, there seemed to be some discrepancy: RBC flow tended to be preserved even after

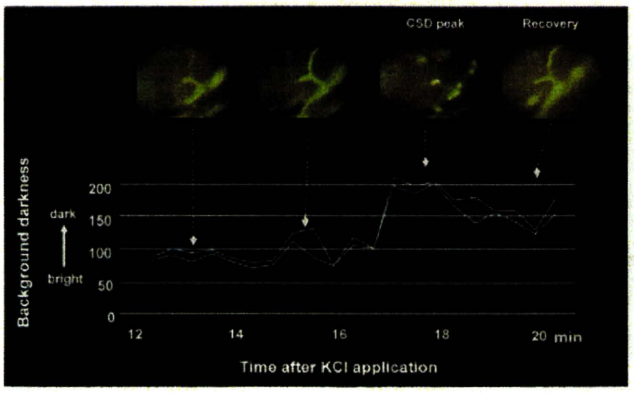

Fig. 10. Background darkness (neuronal depolarization) changes and sample images showing associated RBC movements. In this particular case, there seemed to be a slight discrepancy between the two processes, as the background darkening started before RBC flow decrease became detectable 14 min after KCl application.

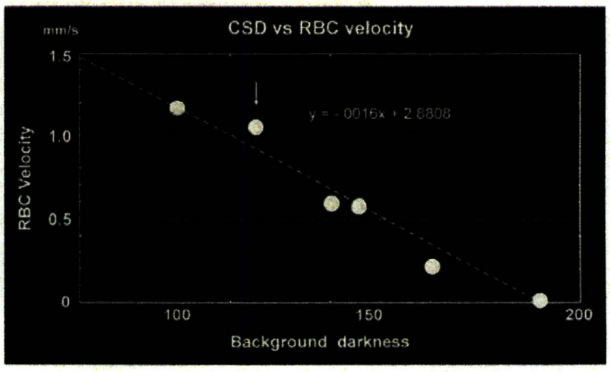

Fig. 11. Linear relationship between changes of tissue background darkness produced by neuronal depolarization and RBC velocity. Again, slowing of RBC flow (arrow) was slightly delayed compared with the start of background darkening.

Please cite this article as: Tomita, M., et al., Oscillating neuro-capillary coupling during cortical spreading depression as observed by tracking of FITC-labeled RBCs in single capillaries, NeuroImage (2011), doi:10.1016/j.neuroimage.2011.02.078

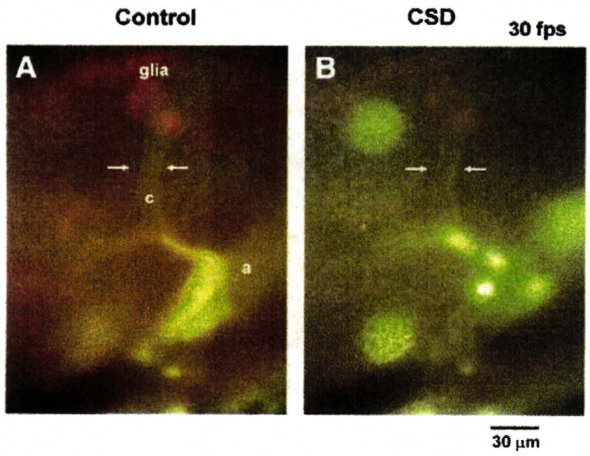

Fig. 12. No change in diameter of capillary occurred in the control period or during CSD, when the RBC velocity in the capillary decreased to less than 1/3 of the control value.

the background darkness started to decrease at 4 min. Such a lag time was often observed (Fig. 10), implying that the intrinsic neuronal depolarization occurred first, followed by a vascular event which was reflected in the change of RBC movements. A linear relationship between the darkness in arbitrary units and RBC velocity was confirmed, as shown in Fig. 11. As indicated by arrows in Fig. 12, there was no detectable change in the diameter of single capillaries between the control state and during CSD. The mechanism of the local slowing-down of RBC velocities was further examined in highly magnified capillaries during CSD passage. Fig. 13 and Supplemental movie 3 show RBCs moving slowly in viscous plasma during the peak of a CSD episode. At time 0, two RBCs were flowing through a capillary channel connecting an arteriole (a: lower) to a venule (v: upper). While the velocities of RBCs in both the arteriole and venule appeared to be rather well maintained, as estimated from RBC elongation, due probably to persisting flows in these vessels, in this short channel the RBC flow became extremely slow. In this sluggish flow, round RBCs in a single capillary (c) showed oscillating motion with occasional stagnation at certain spots, and finally disappeared at 4 or 5 s into the collecting venule. It should be noted that the capillary plasma appeared to be very sludgy and viscous, containing amorphous materials. The buffy coat on the internal surface of the capillary wall appeared to be thickened, continuing to or connecting with the intraluminal amorphous materials. In short, the apparent hemorheological changes were observed to occur in the capillary channels only, and not in inlet or outlet vessels.

Discussion

The findings of this study with our high-speed camera system were that RBC flows in single capillaries under physiological conditions were as high as 2 mm/s (Unekawa et al., 2008), and that flow was not stationary (Mchedlishvili, 1998), but rather high-frequency oscillatory in nature (capillary vasomotion). Employing two-photon microscopy, Kleinheld found that RBC flow in individual capillaries within the specific area sensitive to vibrissae was quite variable with a speed of 0.8 ± 0.5 mm/s and an oscillation frequency of 0.1 Hz in SD rats (Kleinfeld, 2002). When vibrissae were stimulated, the RBC velocity increase was limited to only a 20% increase over the basal velocity, which was comparable to the level of the highest fluctuations seen in single capillaries. According to Kleinfeld, flow increase would therefore be largely masked by basal fluctuations, limiting the sensitivity of brain imaging techniques, at least at low frequencies.

When neurons were depolarized during CSD and became dysfunctional, RBC flow became slower and was rectified, losing its oscillatory character, as described above. Periodic exclusion of RBCs was observed from the capillary network in association with on-going neuronal depolarization (Tomita et al., 2008b). This seems to conflict with the results of Takano et al., who found that CSD induced tissue hypoxia through a transient increase in oxygen demand; there was an increase in capillary flow for several minutes, followed by a relative decrease in mice (Takano et al., 2007b). It was also reported that CSD remarkably enhances CBF to support an increased metabolic rate (Piilgaard and Lauritzen, 2009; Shinohara et al., 1979) and induces mild initial hypoperfusion, followed by transient hyperemia (Ayata et al., 2004) in rats. However, our data are not necessarily in conflict with the above findings. In young rats, no increase in CBF was found in response to CSD, and accompanying transient capillary flow drop was observed, with cessation of RBC flux in 19% of capillaries (Chuquet et al., 2007). We found single capillaries in which RBC flow slowed in response to CSD, among the numerous capillaries examined in this study. We also preliminarily found single capillaries in which RBC flowed fast during the passage of CSD (unpublished data); namely, the flow response to CSD is not uniform.

Within a limited region, the existence of neuro-capillary coupling might be supported by the linear correlation between decrease in RBC

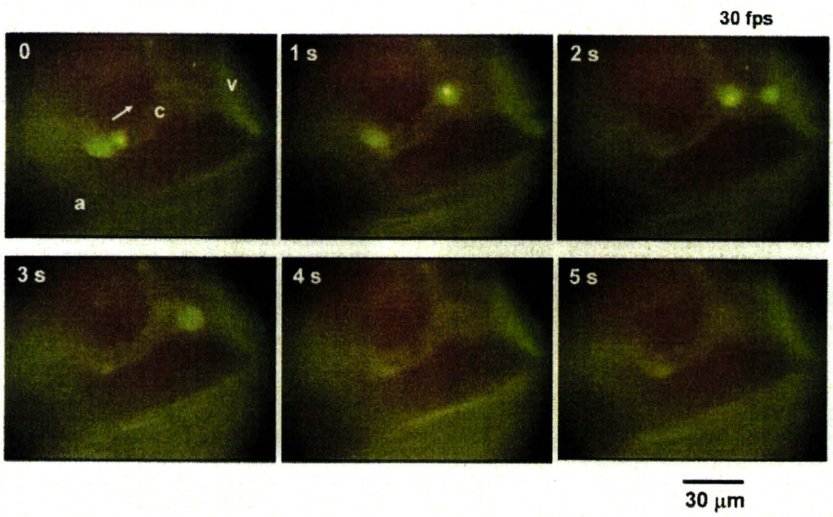

Fig. 13. FITC-labeled RBCs and FITC-stained endothelial cells, observed in a video clip (30 fps) at the peak of CSD (neuronal depolarization). The capillary plasma appeared to be very sludgy and viscous. In such sluggish flow, round RBCs in a single capillary (c) showed a staggering motion, occasionally coming to a full stop. On the other hand, flow in the arteriole and venule was quite well maintained in this case, as estimated from the elongation of flowing RBCs.

Please cite this article as: Tomita, M., et al., Oscillating neuro-capillary coupling during cortical spreading depression as observed by tracking of FITC-labeled RBCs in single capillaries, NeuroImage (2011), doi:10.1016/j.neuroimage.2011.02.078

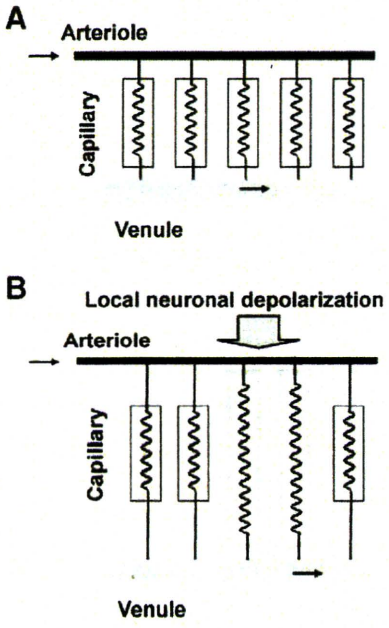

Fig. 14. A parallel capillary model. Top (A) equal resistance to capillary flow in the control state, bottom (B) during CSD, some capillary channels are involved in the propagating wave and the plasma in them becomes highly viscous. RBCs start to detour around the deranged channels.

velocity and change in tissue background darkness. In these circumstances, the flow would not follow Poiseuille's law, which states that the flow rate is proportional to the fourth power of the radius and inversely proportional to viscosity for a Newtonian fluid, and shear rate does not affect the viscosity. Rather, the flow would resemble that of a viscous non-Newtonian fluid, where shear rate does influence the viscosity. Systemic hemodilution increased RBC velocity and RBC flux in capillaries, probably due to reduced blood viscosity or lowered oxygen content. Thus, decrease in blood viscosity seems to be an important factor in the hyperemic response, possibly through a shear stress-dependent mechanism (Hudetz, 1997). Formation of spindle-shaped strings (Osada et al., 2006) or swelling of the neuronal cell body (Takano et al., 2007b) after elicitation of CSD might alter the shear stress in the nearby capillaries. Also, it was demonstrated that NO enhanced leukocyte rolling and modulated leukocyte–endothelial interaction (Lindauer et al., 1996). Locally produced NO might result in changes of local microcirculation, possibly through alteration of blood viscosity. In such cases, change in diameter of capillaries is no longer effective to regulate the flow (Mchedlishvili et al., 2000; Tomita, 2008). The decrease of RBC velocity in capillaries appears to be a local intrinsic event, since it occurs in the absence of any arterial blood pressure change and in the absence of observable diametric change in the upstream feeding arterial systems.

As shown in Fig. 14, RBC flows in all capillaries are regulated individually and independently (top A) in the control state, but when the neurons are depolarized during CSD (bottom B), some channels lose their regulation and the local capillary flow resistance is increased. Flowing RBCs would tend to be excluded from these high flow-resistance channels and would start to detour to other channels with lower flow-resistance.

Conclusions

The observed RBC flow behavior changes in intraparenchymal capillaries during CSD suggest the presence of a regulatory mechanism of cerebral capillary flow, presumably via hemorheological factors, that may involve a direct or indirect coupling between neurons and nearby capillaries via astroglial elements.

Supplementary data associated with this article can be found, in the online version, at doi:10.1016/j.neuroimage.2011.02.078.

The first author, Minoru Tomita, passed away on 17th January 2010. This work was completed by his co-authors.

Acknowledgments

This work was supported by JSPS Grants-in-Aid # 17390255 (Suzuki, N) and # 19591008 (Tomita, Y). The authors also thank Otsuka Pharmaceutical Co., Ltd. for financial support.

References

Anderson, T.R., Andrew, R.D., 2002. Spreading depression: imaging and blockade in the rat neocortical brain slice. J. Neurophysiol. 88, 2713–2725.
Ayata, C., Shin, H.K., Salomone, S., Ozdemir-Gursoy, Y., Boas, D.A., Dunn, A.K., Moskowitz, M.A., 2004. Pronounced hypoperfusion during spreading depression in mouse cortex. J. Cereb. Blood Flow Metab. 24, 1172–1182.
Biswal, B.B., Hudetz, A.G., 1996. Synchronous oscillations in cerebrocortical capillary red blood cell velocity after nitric oxide synthase inhibition. Microvasc. Res. 52, 1–12.
Chaigneau, E., Oheim, M., Audinat, E., Charpak, S., 2003. Two-photon imaging of capillary blood flow in olfactory bulb glomeruli. Proc. Natl. Acad. Sci. U. S. A. 100, 13081–13086.
Chuquet, J., Hollender, L., Nimchinsky, E.A., 2007. High-resolution in vivo imaging of the neurovascular unit during spreading depression. J. Neurosci. 27, 4036–4044.
del Zoppo, G.J., 2010. The neurovascular unit in the setting of stroke. J. Intern. Med. 267, 156–171.
Hudetz, A.G., 1997. Blood flow in the cerebral capillary network: a review emphasizing observations with intravital microscopy. Microcirculation 4, 233–252.
Kleinfeld, D., Mitra, P.P., Helmchen, F., Denk, W., 1998. Fluctuations and stimulus-induced changes in blood flow observed in individual capillaries in layers 2 through 4 of rat neocortex. Proc. Natl. Acad. Sci. U. S. A. 95, 15741–15746.
Kleinfeld, D., Denk, W., 2000. Two-photon imaging of neocortical microcirculation. In: Yuste, R., Lanni, F., Konnerth, A. (Eds.), Imaging Neurons: A Laboratory Manual. Cold Spring Harbor Laboratory Press, Cold Spring Harbor, pp. 23.10–23.15.
Kleinfeld, D., 2002. Cortical blood flow through individual capillaries in rat vibrissa S1 cortex: stimulus-induced changes in flow are comparable to the underlying fluctuations in flow. In: Tomita, M., Kanno, I., Hamel, E. (Eds.), Brain Activation and CBF Control; Exerpta Medica International Congress Series 1235. Elsevier Science, Amsterdam, pp. 115–122.
Krogh, A., 1919. The supply of oxygen to the tissues and the regulation of the capillary circulation. J. Physiol. 52, 457–474.
Leão, A., 1944. Spreading depression of activity in cerebral cortex. J. Neurophysiol. 7, 359–390.
Lindauer, U., Dreier, J., Angstwurm, K., Rubin, I., Villringer, A., Einhaupl, K.M., Dirnagl, U., 1996. Role of nitric oxide synthase inhibition in leukocyte–endothelium interaction in the rat pial microvasculature. J. Cereb. Blood Flow Metab. 16, 1143–1152.
Mchedlishvili, G., 1986. Arterial behavior and blood circulation in the brain. Plenum Press, New York.
Mchedlishvili, G., 1998. Disturbed blood flow structuring as critical factor of hemorheological disorders in microcirculation. Clin. Hemorheol. Microcirc. 19, 315–325.
Mchedlishvili, G., Tomita, M., Schmid-Sconbein, G.W., 2000. Hemorrheology in microcirculation: pathological changes. Internet Virtual Symposium, the 7th Tbilisi Symposium. Keio J. Med., 49 (Suppl. 3). Keio University, Tokyo.
Nakai, K., Imai, H., Kamei, I., Itakura, T., Komari, N., Kimura, H., Nagai, T., Maeda, T., 1981. Microangioarchitecture of rat parietal cortex with special reference to vascular "sphincters." Scanning electron microscopic and dark field microscopic study. Stroke 12, 653–659.
Nimmerjahn, A., Kirchhoff, F., Kerr, J.N., Helmchen, F., 2004. Sulforhodamine 101 as a specific marker of astroglia in the neocortex in vivo. Nat. Methods 1, 31–37.
Osada, T., Tomita, M., Suzuki, N., 2006. Spindle-shaped constriction and propagated dilation of arterioles during cortical spreading depression. NeuroReport 17, 1365–1368.
Piilgaard, H., Lauritzen, M., 2009. Persistent increase in oxygen consumption and impaired neurovascular coupling after spreading depression in rat neocortex. J. Cereb. Blood Flow Metab. 29, 1517–1527.
Schiszler, I., Tomita, M., Fukuuchi, Y., Tanahashi, N., Inoue, K., 2000. New optical method for analyzing cortical blood flow heterogeneity in small animals: validation of the method. Am. J. Physiol. 279, H1291–H1298.
Seylaz, J., Charbonné, R., Nanri, K., Von Euw, D., Borredon, J., Kacem, K., Méric, P., Pinard, E., 1999. Dynamic in vivo measurement of erythrocyte velocity and flow in capillaries and of microvessel diameter in the rat brain by confocal laser microscopy. J. Cereb. Blood Flow Metab. 19, 863–870.
Shinohara, M., Dollinger, B., Brown, G., Rapoport, S., Sokoloff, L., 1979. Cerebral glucose utilization: local changes during and after recovery from spreading cortical depression. Science 203, 188–190.
Takano, T., Han, X., Deane, R., Zlokovic, B., Nedergaard, M., 2007a. Two-photon imaging of astrocytic Ca^{2+} signaling and the microvasculature in experimental mice models of Alzheimer's disease. Ann. NY Acad. Sci. 1097, 40–50.

Takano, T., Tian, G.F., Peng, W., Lou, N., Lovatt, D., Hansen, A.J., Kasischke, K.A., Nedergaard, M., 2007b. Cortical spreading depression causes and coincides with tissue hypoxia. Nat. Neurosci. 10, 754–762.

Tomita, M., Gotoh, F., Sato, T., Tanahashi, N., Tanaka, K., 1981. 4–6 Cycle per minute fluctuation in cerebral blood volume of feline cortical tissue in situ. J. Cereb. Blood Flow Metab. 1 (Suppl 1), S443–S444.

Tomita, M., Fukuuchi, Y., Terakawa, S., 1994. No appreciable swelling of cultured neurons after oxygen deprivation, and cell damage occasionally aggravated by oxygen resupply. In: Hartmann, A., Yatsu, Y., Kuschinsky, W. (Eds.), Cerebral Ischemia and Basic Mechanisms. Springer-Verlag, Berlin Heidelberg, pp. 273–280.

Tomita, M., Schiszler, I., Tomita, Y., Tanahashi, N., Takeda, H., Osada, T., Suzuki, N., 2005a. Initial oligemia with capillary flow stop followed by hyperemia during K^+-induced cortical spreading depression in rats. J. Cereb. Blood Flow Metab. 25, 742–747.

Tomita, M., 2008. Basic mechanisms of brain ischemia; minireview on microcirculation capillo-venous flow disturbances in brain ischemia. In: Erdõ, F. (Ed.), Recent Advances and New Strategies in Stroke Research. Transworld Research Network, Kerala, India, pp. 91–112.

Tomita, M., Osada, T., Schiszler, I., Tomita, Y., Unekawa, M., Toriumi, H., Tanahashi, N., Suzuki, N., 2008a. Automated method for tracking vast numbers of FITC-labeled RBCs in microvessels of rat brain in vivo using a high-speed confocal microscope system. Microcirculation 15, 163–174.

Tomita, M., Tomita, Y., Osada, T., Unekawa, M., Toriumi, H., Tatarishvili, J., Suzuki, N., 2008b. Periodic disappearance of RBC from focal capillary network during K^+-induced cortical spreading depression in rodents. J. Vasc. Res. 45 (Suppl. 2), 65.

Tomita, M., Osada, T., Unekawa, M., Tomita, Y., Toriumi, H., Suzuki, N., 2009a. Exogenous nitric oxide increases microflow but decreases RBC attendance in single capillaries in rat cerebral cortex. Microvasc. Rev. Commun. 3, 11–16.

Tomita, M., Tomita, Y., Toriumi, H., Unekawa, M., Suzuki, N., 2009b. Coupling of capillary RBC flow failure with neuronal depolarization. Nature Proceedings. The data are available at http://precedings.nature.com/documents/3220/version/1.

Tomita, Y., Tomita, M., Schiszler, I., Amano, T., Tanahashi, N., Kobari, M., Takeda, H., Ohtomo, M., Fukuuchi, Y., 2002. Repetitive concentric wave-ring spread of oligemia/hyperemia in the sensorimotor cortex accompanying K^+-induced spreading depression in rats and cats. Neurosci. Lett. 322, 157–160.

Tomita, Y., Kubis, N., Calando, Y., Tran Dinh, A., Méric, P., Seylaz, J., Pinard, E., 2005b. Long-term in vivo investigation of mouse cerebral microcirculation by fluorescence confocal microscopy in the area of focal ischemia. J. Cereb. Blood Flow Metab. 25, 858–867.

Unekawa, M., Tomita, M., Osada, T., Tomita, Y., Toriumi, H., Tatarishvili, J., Suzuki, N., 2008. Frequency distribution function of red blood cell velocities in single capillaries of the rat cerebral cortex using intravital laser-scanning confocal microscopy with high-speed camera. Asian Biomed. 2, 203–218.

Unekawa, M., Tomita, M., Tomita, Y., Toriumi, H., Hattori, H., Suzuki, N., 2009. Shift of frequency distribution of RBC velocity in parenchymal capillaries during potassium-induced cortical spreading depression in rats. J. Cereb. Blood Flow Metab. 29, S298.

Unekawa, M., Tomita, M., Tomita, Y., Toriumi, H., Miyaki, K., Suzuki, N., 2010. RBC velocities in single capillaries of mouse and rat brains are the same, despite 10-fold difference in body size. Brain Res. 1320, 69–73.

Villringer, A., Them, A., Lindauer, U., Einhäupl, K., Dirnagl, U., 1994. Capillary perfusion of the rat brain cortex. An in vivo confocal microscopy study. Circ. Res. 75, 55–62.

Vogel, J., Abounader, R., Schrock, H., Zeller, K., Duelli, R., Kuschinsky, W., 1996. Parallel changes of blood flow and heterogeneity of capillary plasma perfusion in rat brains during hypocapnia. Am. J. Physiol. 270, H1441–H1445.

Wolf, J., 1970. Anchorage of collagenous fibrils in brain surface wrapping basal membrane (membrana limitans gliae superficialis). Folia Morphol. Praha 18, 322–329.

Yanamoto, K., Hosoi, R., Uesaka, Y., Abe, K., Tsukada, H., Inoue, O., 2003. Intrastriatal microinjection of sodium nitroprusside induces cell death and reduces binding of dopaminergic receptors. Synapse 50, 137–143.

Please cite this article as: Tomita, M., et al., Oscillating neuro-capillary coupling during cortical spreading depression as observed by tracking of FITC-labeled RBCs in single capillaries, NeuroImage (2011), doi:10.1016/j.neuroimage.2011.02.078